Hindawi Publishing Corporation
Journal of Nanoscience
Volume 2013, Article ID 587345, 6 pages
http://dx.doi.org/10.1155/2013/587345

Research Article

Connected Lead Zirconate Titanate Nanodot Arrays for Perspective Functional Materials

M. Waegner,[1] A. Finn,[2] G. Suchaneck,[1] G. Gerlach,[1] and L. M. Eng[3]

[1] *Solid State Electronics Laboratory, Technische Universität Dresden, 01062 Dresden, Germany*
[2] *Institute of Semiconductor and Microsystems Technology, Technische Universität Dresden, 01062 Dresden, Germany*
[3] *Institute of Applied Photophysics, Technische Universität Dresden, 01062 Dresden, Germany*

Correspondence should be addressed to M. Waegner; martin.waegner@mailbox.tu-dresden.de

Received 25 March 2013; Accepted 29 May 2013

Academic Editor: Faming Zhang

Copyright © 2013 M. Waegner et al. This is an open access article distributed under the Creative Commons Attribution License, which permits unrestricted use, distribution, and reproduction in any medium, provided the original work is properly cited.

We describe the fabrication of lead zirconate titanate (PZT) nanodisc arrays isolated by a polymer layer and contacted with a top electrode. PZT thin films were deposited by multitarget sputtering onto a platinum/titanium bottom electrode and structured by means of nanosphere lithography. To guarantee short-circuit-free deposition of a top electrode, the space between the nanostructures was filled by a polymer. Two approaches for the filling are demonstrated: (a) imprinting and (b) skim coating. Single nanodiscs embedded in a flexible polymer matrix have two major advantages. First, taking into account the flexibility of the matrix, they can vibrate in lateral direction and, second, due to shrinking to the nanoscale, predominant directions of the polarization form, such as vortex- or bubble-like domain patterns. Piezoresponse force microscopy was performed on patterned and nonpatterned samples with and without a top electrode to check the local piezoresponse. Comparison of the different samples revealed an increase in lateral piezoactivity for patterned samples with Ni/Cr electrode while the out-of-plane piezoresponse remained constant. Gold electrodes limit the piezoresponse in both measured directions.

1. Introduction

Ferroelectric thin films are of important interest in microelectromechanical systems (MEMS). Especially PZT films combined with a standard CMOS process result in novel sensor and actuator devices like accelerometers [1], pressure sensors [2], motors [3], and ultrasonic transducers [4].

For further improvement of these devices, current research looks for novel functional materials with enhanced sensitivity or additional properties like flexibility and elasticity. Therefore, nanopatterning is an ideal technique to improve properties of ferroelectric materials. Enhanced material coefficients in ferroelectric nanopowders were already found in the 1950s [5]. But still today the reasons for the increase in pyro- and piezoelectric coefficients are under discussion. Taking advantage of this effect offers a large variety of perspective applications. Recently, remarkable increases in the local piezoresponse of nanopatterned PZT films were observed, both in the plane as well as out of the plane. This effect is mainly driven by the aspect ratio of the nanostructures [6]. More precisely, the enhancement is caused by the breakup of grains in order to compensate the stress induced by the polarization field and depends on the lateral dimensions and aspect ratio of the structures. By connecting such nanostructures equal in polarization and piezoresponse to arrays, more sensitive materials might result.

In this work, we describe the fabrication of well-defined ferroelectric nanodisc arrays isolated by a matrix resist and connected on top via a common electrode without short-circuiting top and bottom electrode. Changes in local piezoresponse were investigated by piezoresponse force microscopy (PFM).

2. Experimental

2.1. Material. A Si/SiO_2 wafer with a (111)-oriented platinum/titanium bottom electrode was used as starting material. Tetragonal $Pb(Zr_{0.3}Ti_{0.7})O_3$ (PZT) was deposited by

reactive multitarget magnetron sputtering yielding polycrystalline, highly (111)-textured PZT thin films with a thickness of about 120 nm [7].

2.2. Nanopatterning Process. The wafer was cut into small pieces of $5 \times 5\,\text{mm}^2$ and the samples were patterned by means of nanosphere lithography (NSL) [8]. Polystyrene nanosphere monolayers self-assembled on the surface of the PZT samples were used as a mask for ion milling. This dry etching technique transfers the mask 1 : 1 to the ferroelectric thin film yielding in a nanopatterned layer built up of regular-ordered nanodiscs with a narrow diameter distribution and well-defined pitch. Further details of this technique can be found elsewhere [9].

2.3. Filling the Voids. To prevent short-circuits between the top and the bottom electrode the voids between the nanodiscs were filled by a flexible matrix. Two approaches were applied: (a) imprinting [10] and (b) skim coating. For both approaches the samples were cleaned in acetone and deionized water and, finally, treated in low-pressure oxygen plasma to ensure a clean, hydrophilic surface.

(a) Imprinting. The imprint process is sketched in Figure 1(b). A flexible stamp was cast from a bare polished silicon wafer [11]. Perfluoropolyether (PFPE) Fluorolink MD700 (Solvay Solexis) was used as a stamp material. The small patterned sample was placed in a custom-built imprint press and $2\,\mu\text{L}$ of mr-UVCur21SF resist (micro resists technology) was dispensed on it. Afterwards, the flat stamp was imprinted on the patterned sample and the polymer which was not required to fill the voids was squeezed out. The resist was cured directly through the stamp by using a UV-LED source (365 nm, $300\,\text{mW/cm}^2$) for 2 min. Figure 1(c) shows a micrograph of a nanopatterned PZT layer with polymer imprinted in between the nanodiscs. The imprint pressure and the flexibility of the stamp were optimized yielding imprints without a residual layer on the dots' top. Residual layers covering the whole sample can be also removed by a short oxygen plasma etching step.

Achieving imprints without residual layers on the dots' top is the the most challenging part of this technology which can be overcome by optimizing the imprint pressure and elasticity of the imprint stamp.

(b) Skim Coating. Polyethylene glycol diacrylate (PEGDA) with 0.5% Irgacure 651 as a photo-initiator was used to skim coat nanopatterned samples. The small sample was fixed on a vacuum chuck and PEGDA solution was dispensed until it was completely covered. Skimming of the remaining resist was done with the help of a PDMS squeegee (Figure 1(d)). Depending on the contact pressure and the amount of remaining resist, the process has to be repeated. The skim coat was successful when the surface looks homogeneously covered without any interference. The resist was finally cured using UV light ($\lambda = 365\,\text{nm}$) for 10 min. Figure 1(e) shows a micrograph of a nanodisc array filled with PEGDA. It can be seen that areas with nonperfect ordering of nanodiscs, meaning an increased pitch between the dots, might not be completely covered by the resist. This is caused by the flexible PDMS squeegee which is pressed down to the residual layer when the pitch between the nanodiscs becomes too large. Investigations with a scanning force microscope revealed the formation of polymeric rings around the nanodots (Figure 2(b)). A very thin residual layer of PEDGA is also covering the tops of the nanodots with a height of about 10 nm. During the UV-curing the surface tension increases and the thin residual layer rips apart and forms the small rings around the nanodots. On the one hand side, this effect increases the surface roughness, but on the other hand, a direct contact of the evaporated electrode with the the tops of the nanodots is guaranteed.

After filling the voids small electrodes of nickel chromium (80 : 20) or gold were evaporated through a shadow mask onto the isolated nanodots. The squared electrodes are about 15 μm in length and have a thickness of about 10 nm. Figure 2(a) shows a micrograph of a nanopatterned layer partly covered by an Au electrode (bright area). The sheet resistance for 10 nm Ni/Cr and Au on glass was 315 Ω and 6.8 Ω, respectively.

2.4. Measurement of Local Piezoelectric Response. An AIST-NT SmartSPM in PFM mode was used as the inspection tool for local piezoresponse measurements. Standard soft ($k \approx 0.1\,\text{N/m}$; $f_{\text{res}} \approx 20\,\text{kHz}$) and hard ($k \approx 2.5\,\text{N/m}$; $f_{\text{res}} \approx 150\,\text{kHz}$) cantilevers with a conductive TiN coating were used to measure both the in-plane and out-of-plane amplitude and phase. The different cantilevers revealed qualitatively similar results. The tip was driven by an excitation voltage $U_{\text{pp}} = 6\,\text{V}$ at a frequency of 48.1 kHz.

3. Discussion

First, nonpatterned samples were studied. Figures 3(a)–3(c) show a closed PZT thin film with a thickness of about 120 nm, which was partly covered by a Ni/Cr electrode in the upper right part. It is clearly seen that the electrode limits the degree of freedom of vibrations induced by the local piezoresponse for both in-plane and out-of-plane direction. While the single grains of the uncovered PZT film have a large averaged local piezoresponse with parts of high activity (bright color) and parts of low to zero activity (dark color), the contrast in the area covered by an electrode is very weak (Figures 3(b) and 3(c)). The domains are still visible but they are limited in their response in both measured directions. This is caused on the one hand side by an additional clamping effect of the electrode and on the other hand side by the loss of the highly localized response in PFM due to the conductive electrode. When applying the AC voltage of the conductive PFM tip at the electrode, a large area of polycrystalline grains responds to the excitation. Adjacent grains, which normally have opposite phase, are no longer able to move into different directions because they are clamped by the top electrode.

The behavior of nanopatterned films was studied by the same method. Figures 3(e)-3(f) show both the resulting topography and PFM amplitude images. The surface is

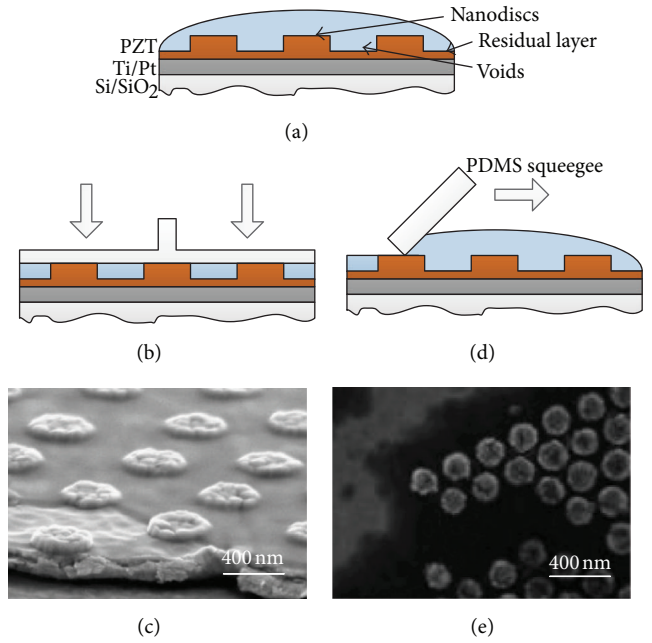

Figure 1: Filling of voids between nanostructures: (a) nano-nanopatternedpatterned starting material with monomer solution, (b) imprinting with (c) side view micrograph of imprinted polymer, and (d) skim coating with (e) top view micrograph of resulting structures. The dark surrounding material is PEGDA.

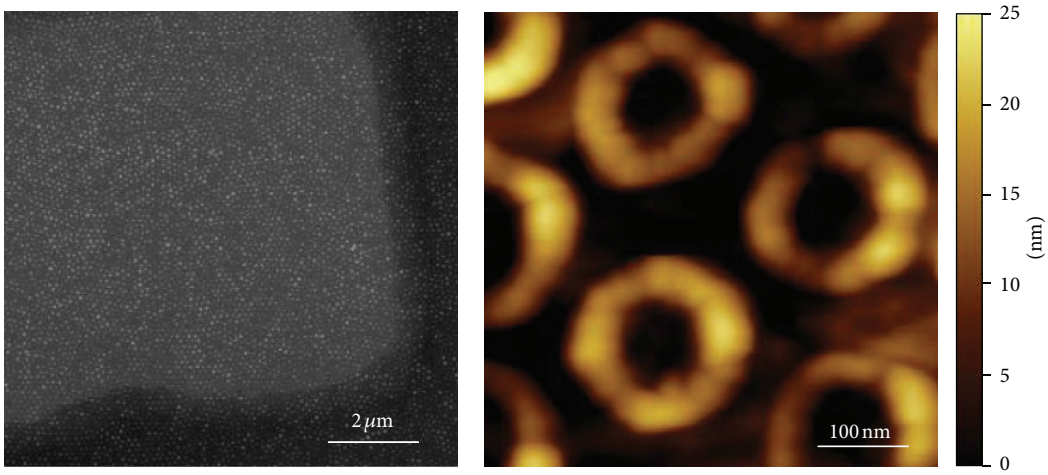

Figure 2: PZT nanodot array: (a) micrograph of the array with filled voids and covered by an Au electrode (bright part) and (b) AFM topography image of the array filled with PEDGA by means of skim coating.

rougher due to the nanopatterning. The nanodiscs are 100–300 nm in diameter and 80 nm in height and are arranged on a 40 nm closed residual layer of PZT (Figure 1(a)). The regular ordering of the nanodiscs can be seen in the topography as well as in the out-of-plane image. Interestingly, the evaporation of an Ni/Cr electrode does not limit the piezoresponse in both directions. For the out-of-plane direction the averaged piezoresponse of the part covered by an electrode (Figure 3(e); darker part) and the part with an electrode is nearly unchanged. However, there is an overall increase in the averaged amplitude in the in-plane direction. This can be seen in Figure 3(f) where the area with electrode appears brighter, what is caused by a higher local piezoactivity.

The electrodes clamp again the tops of the nanodiscs, resulting in a limitation of local vibrations in the normal out-of-plane direction. Contrarily, the lateral in-plane direction is not clamped. In the voids between the discs the resist works like a buffer which does not completely suppress the in-plane

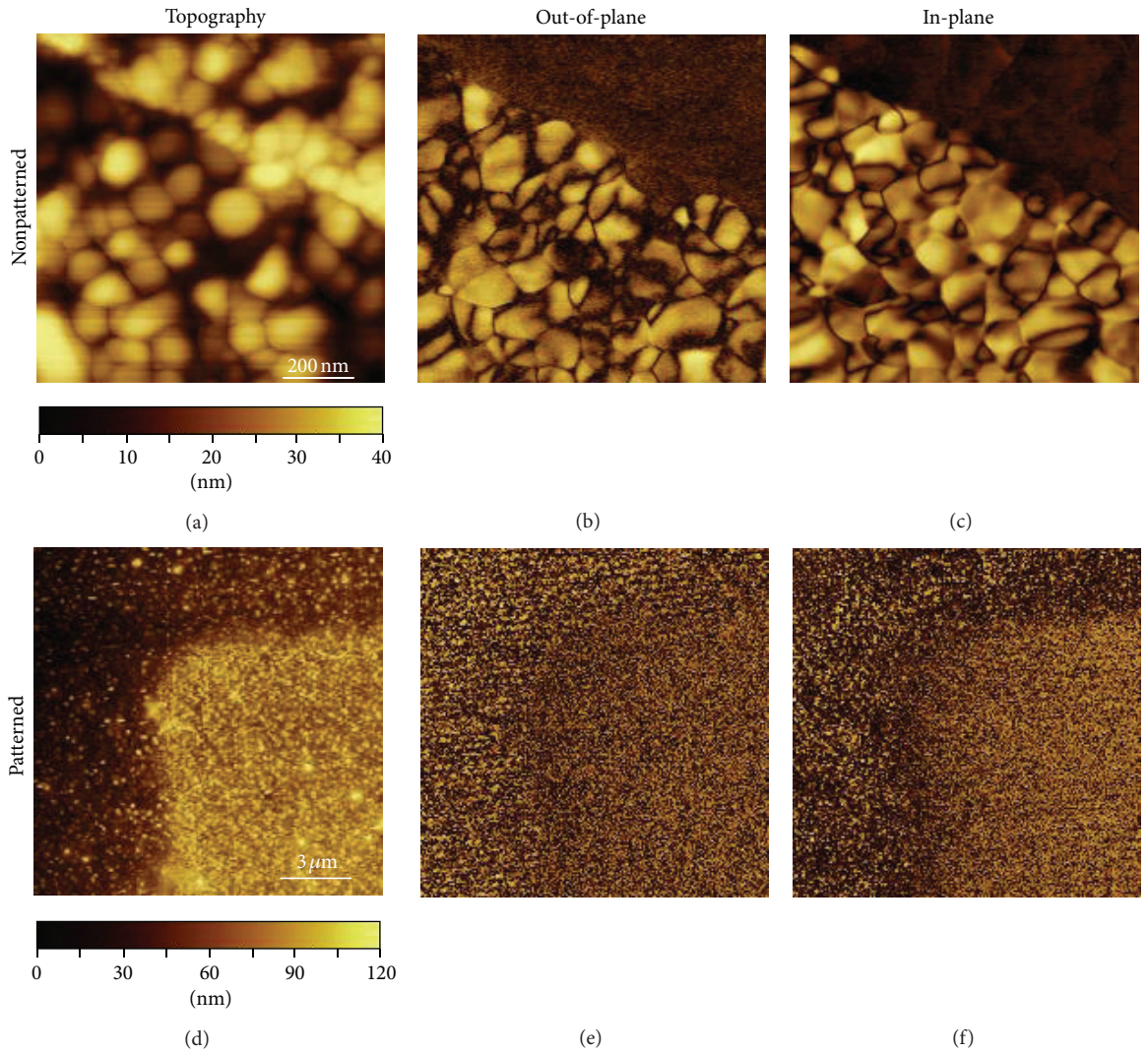

Figure 3: Nonpatterned PZT thin film (a)–(c) with an evaporated Ni/Cr electrode in the upper right part and nanopatterned PZT thin film (disc diameter ≈ 300 nm, disc height ≈ 80 nm) (d)–(f) with filled voids and an evaporated Ni/Cr electrode in the lower right part: (a), (d) topography, (b), (e) out-of-plane, and (c), (f) in-plane amplitude PFM images.

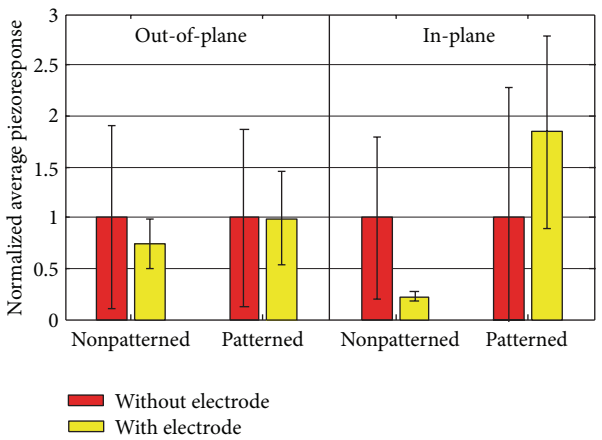

Figure 4: Averaged local piezoelectric response opposing nonpatterned/patterned films with and without electrode both in-plane and out-of-plane.

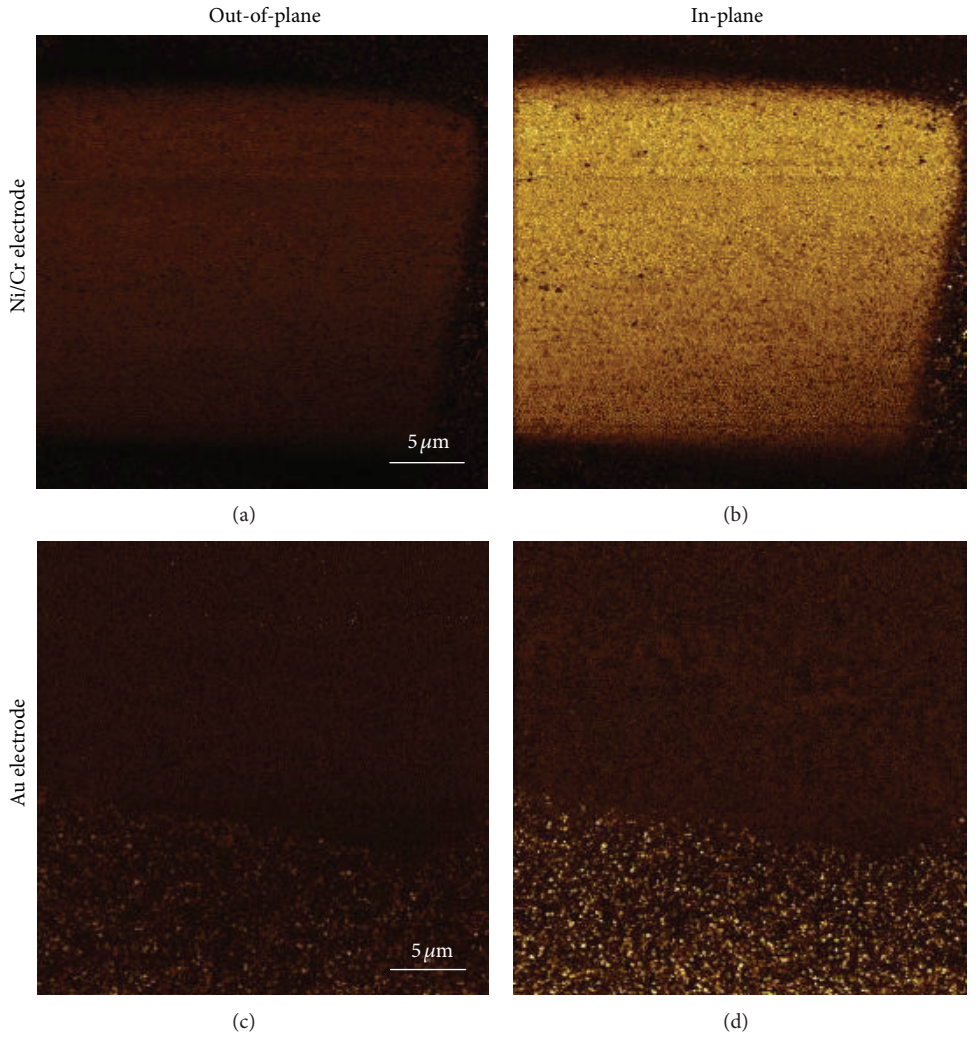

FIGURE 5: (a), (c) Out-of-plane (b), (d) and in-plane amplitude PFM images of a nanopatterned film (disc diameter ≈ 100 nm, disc height ≈ 80 nm) with filled voids and connected by (a), (b) a Ni/Cr electrode and (c), (d) an Au electrode. Note that the value range for the out-of-plane and in-plane amplitude was equalized for Ni/Cr and Au electrode, respectively, for better comparability.

movement. Furthermore, a homogenous field distribution below the electrode promotes a uniform excitation of the nanostructures below. The average piezoelectric activity over an area was evaluated for both patterned and nonpatterned samples. Figure 4 shows the normalized averaged response for in-plane and out-of-plane measurements of opposing areas with and without Ni/Cr electrode of the sample shown in Figure 3. For nonpatterned samples the averaged piezoactivity decreases to 80% and 20% for out-of-plane and in-plane, respectively. For patterned samples the out-of-plane piezoresponse is not affected by the electrode, but the in-plane response is remarkably increased and reaches almost 200% for discs with a diameter of about 300 nm. Comparing patterned and nonpatterned films, each with an electrode, with respect to the out-of-plane direction, the difference is negligible. The continuous film or the tops of the nanodiscs are clamped by the electrode and prevent free local vibrations. Comparing the in-plane direction of both films, the nanodiscs are not clamped laterally and lateral movement is not restricted as in a continuous film. This effect can be used to enhance the lateral sensitivity of perspective sensor materials.

Figure 5 shows the amplitude images of the local piezoresponse for smaller nanodots with a diameter of about 100 nm. The same sample was partly covered by small Ni/Cr electrodes and partly by Au electrodes. The investigation of nanodot arrays connected through a directly deposited Au electrode revealed neither for in-plane nor for out-of-plane direction an increase of locale piezoresponse. The value remained constant or was decreased. We attribute this effect to the higher density of gold which causes a higher damping of the piezoresponse. Measurements on the same sample with a Ni/Cr electrode showed an increase for both measured directions. Comparing the averaged local piezoelectric

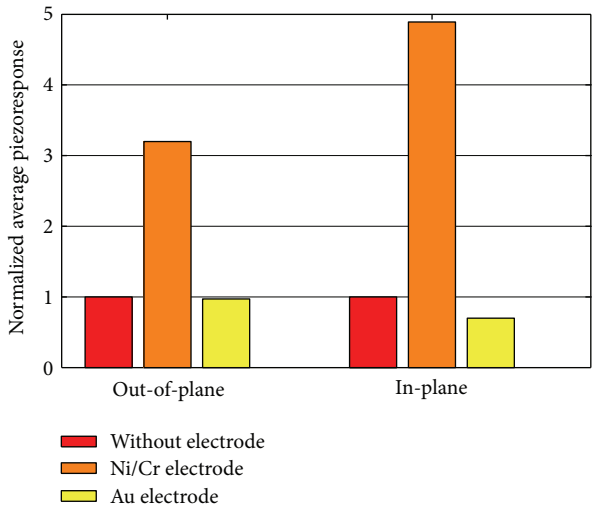

Figure 6: Averaged local piezoelectric response opposing nonpatterned/patterned films with and without electrode both in-plane and out-of-plane.

response with arrays consisting of larger discs (Figure 4), the in-plane amplitude is further increased (Figure 6). This was already observed on single nanodots where the average piezoresponse of a single dot increases with increasing aspect ratio [6].

4. Conclusions

A new technique for the fabrication of nanopatterned ferroelectric material was demonstrated. Single nanodiscs, which showed increased piezoelectric response, were connected via a top electrode to use the increased response of a nanodisc array. Deposition of an electrode onto nonpatterned films reduces the piezoresponse due to clamping and reduced flexibility between adjacent domains. In contrast, for patterned films with a Ni/Cr electrode, a strong increase for the in-plane response was measured, while the out-of-plane piezoresponse changes less significant or remains constant. For gold electrodes this effect was not observed. The direct deposition of an Au electrode decreases the in-plane as well as the out-of-plane-response, probably due to a higher damping of the piezoelectric vibration.

Acknowledgment

This work was supported by the German Research Foundation (DFG), Research Training Group 1401 "Nano and Biotechnologies for Packaging of Electronic Systems".

References

[1] K. Kunz, P. Enoksson, and G. Stemme, "Highly sensitive triaxial silicon accelerometer with integrated PZT thin film detectors," *Sensors and Actuators A*, vol. 92, no. 1–3, pp. 156–160, 2001.

[2] M. Olfatnia, T. Xu, J. M. Miao, L. S. Ong, X. M. Jing, and L. Norford, "Piezoelectric circular microdiaphragm based pressure sensors," *Sensors and Actuators A*, vol. 163, no. 1, pp. 32–36, 2010.

[3] M. A. Dubois and P. Muralt, "PZT thin film actuated elastic fin micromotor," *IEEE Transactions on Ultrasonics, Ferroelectrics and Frequency Control*, vol. 45, pp. 1169–1177, 1998.

[4] J. J. Bernstein, S. L. Finberg, K. Houston et al., "Micromachined high frequency ferroelectric sonar transducers," *IEEE Transactions on Ultrasonics, Ferroelectrics, and Frequency Control*, vol. 44, no. 5, pp. 960–969, 1997.

[5] M. Anliker, H. R. Brugger, and W. Kaenzig, "Das Verhalten von kolloidalen Seignettealektrika III, Barium Titanat $BaTiO_3$," *Helvetica Physica Acta*, vol. 27, p. 99, 1954 (German).

[6] M. Waegner, M. Schröder, G. Suchaneck et al., "Enhanced piezoelectric response in nano-patterned lead zirconate titanate thin films," *Japanese Journal of Applied Physics*, vol. 51, 5 pages, 2012.

[7] V. S. Vidyarthi, W.-M. Lin, G. Suchaneck, G. Gerlach, C. Thiele, and V. Hoffmann, "Plasma emission controlled multi-target reactive sputtering for in-situ crystallized $Pb(Zr,Ti)O_3$ thin films on 6″ Si-wafers," *Thin Solid Films*, vol. 515, no. 7-8, pp. 3547–3553, 2007.

[8] M. Waegner, "Nanosphere lithography," in *Bio and Nano Packaging Techniques for Electron Devices*, G. Gerlach and K. J. Wolter, Eds., chapter 12, pp. 269–277, Springer, Berlin, Germany, 2012.

[9] M. Waegner, G. Suchaneck, and G. Gerlach, "Top-down fabrication of ordered mesoscopic PZT dot arrays by natural lithography," *Integrated Ferroelectrics*, vol. 123, no. 1, pp. 75–80, 2011.

[10] A. S. P. Chang, C. Peroz, X. Liang, S. Dhuey, B. Harteneck, and S. Cabrini, "Nanoimprint planarization of high aspect ratio nanostructures using inorganic and organic resist materials," *Journal of Vacuum Science and Technology B*, vol. 27, no. 6, pp. 2877–2881, 2009.

[11] A. Finn, R. Hensel, F. Hagemann, R. Kirchner, A. Jahn, and W. J. Fischer, "Geometrical properties of multilayer nano-imprint-lithography molds for optical applications," *Microelectronic Engineering*, vol. 98, pp. 284–287, 2012.

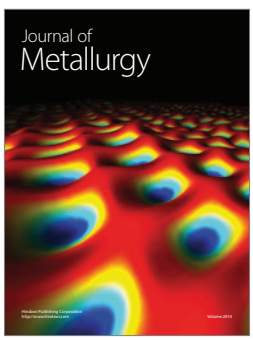

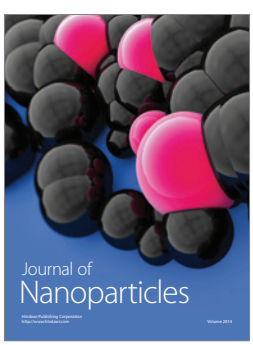

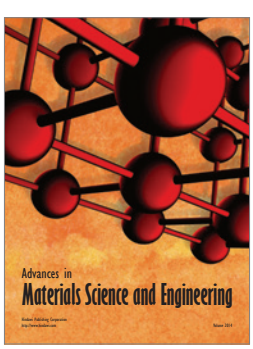

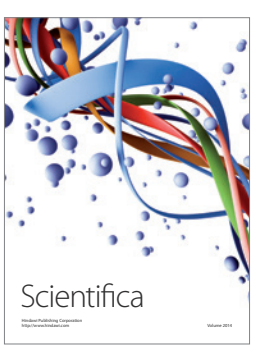

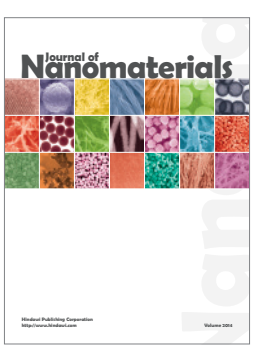

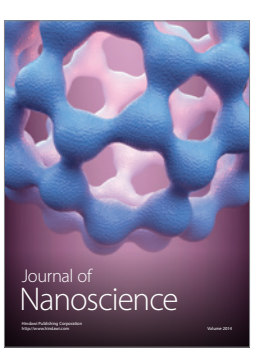

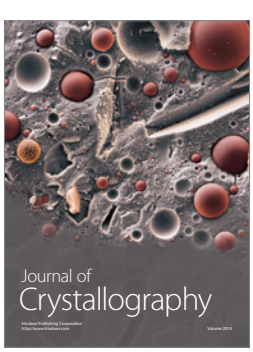

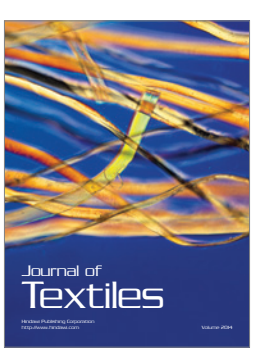

Hindawi

Submit your manuscripts at
http://www.hindawi.com